Electronic Supplementary Material (ESI) for Inorganic Chemistry Frontiers.

Yellow-Emissive Copper(I)-halide Single Crystals with $[Cu_4I_4]$ Cubane Unit as Efficient X-ray Scintillators

Qingzheng Kong,[‡,a] Xiaomei Jiang,[‡,*a] Ying Sun[a], Jianguo Zhu[a] and Xutang Tao[*b]

[a] School of Preventive Medicine Sciences (Institute of Radiation Medicine), Shandong First Medical University & Shandong Academy of Medical Sciences, No. 6699 Qingdao Road, Jinan n 250117, People's Republic of China

[b] School of Crystal Materials (State Key Laboratory of Crystal Materials), Shandong University, No. 27 Shanda South Road, Jinan 250100, People's Republic of China

[‡]These authors contributed equally.

***Corresponding authors.**

E-mail addresses: jiangxiaomei@sdfmu.edu.cn, txt@sdu.edu.cn

Table S1. Crystal and Refinement Data for $(4\text{-bzpy})_4Cu_4I_4$, $(4\text{-bzpy})_2Cu_6I_8$ and $(4\text{-bzpy})_3Cu_3I_6$.

Empirical Formula	$(4\text{-bzpy})_4Cu_4I_4$	$(4\text{-bzpy})_2Cu_6I_8$	$(4\text{-bzpy})_3Cu_3I_6$
Formula Weight/g·mol^{-1}	1438.63	1735.88	1462.7
Crystal System	monoclinic	orthorhombic	monoclinic
Space Group	$P2_1/c$(14)	$P2_12_12_1$(19)	$P2_1/n$(11)
Unit Cell Dimensions	a=18.429(4)Å b=22.752(6)Å c=24.015(6)Å α=γ=90° β=92.281(9)°	a=14.3825(4)Å b=14.7650(5)Å c=17.2330(6)Å α=β=γ=90°	a=6.6180(3)Å b=25.1998(11)Å c=26.4843(14)Å α=γ=90° β=96.387(2)°
Volume/Å^3	10061(5)	3659.56(20)	4389.43(36)
$\rho_{calculated}$/g·mol^{-1}	1.89934	3.15046	2.21325
Z	4	4	4
Completeness to θ = 25	100%	100%	100%
Goodness-of-Fit	1.055	1.037	1.023
Final R Indices [I > 2σ(I)]	R_{obs}=0.0685 ωR_{obs}=0.0879	R_{obs}= 0.0346 ωR_{obs}=0.0548	R_{obs}=0.0748 ωR_{obs}=0.0878
R Indices [all data]	R_{all}=0.1457 ωR_{all}=0.1023	R_{all}= 0.0460 ωR_{all}=0.0583	R_{all}=0.1809 ωR_{all}=0.1068
CCDC Number	1476241[1]	2260238 [This work]	2350403 [This work]

[1]Yang Fang, Wei Liu, Simon Teat, Litao An, Dechao Yu, Jing Li CCDC 1476241: Experimental Crystal Structure Determination, 2017, DOI: 10.5517/ccdc.csd.cc1lk4pz.

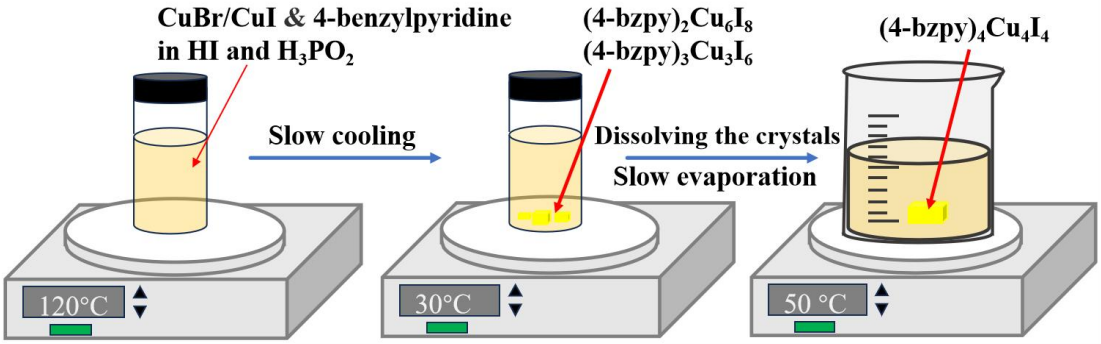

Fig. S1. Schematic diagram of the synthesis of $(4\text{-bzpy})_4Cu_4I_4$, $(4\text{-bzpy})_2Cu_6I_8$ and $(4\text{-bzpy})_3Cu_3I_6$ single crystals.

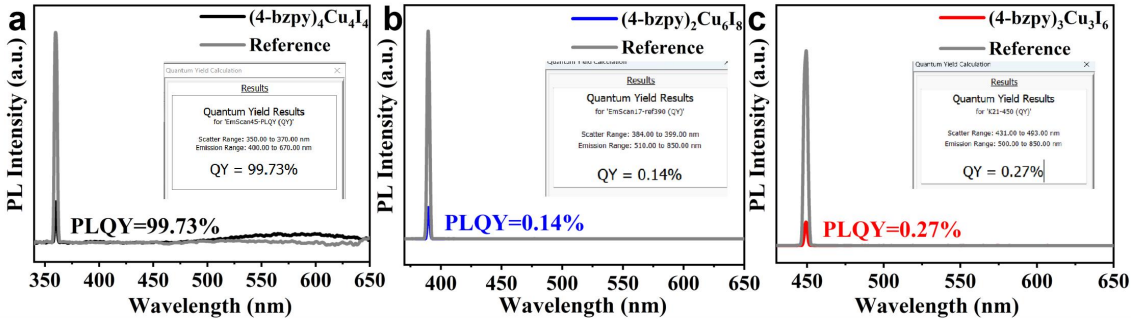

Fig. S2. PLQY measurements of $(4\text{-bzpy})_4Cu_4I_4$, $(4\text{-bzpy})_2Cu_6I_8$ and $(4\text{-bzpy})_3Cu_3I_6$ single crystals.

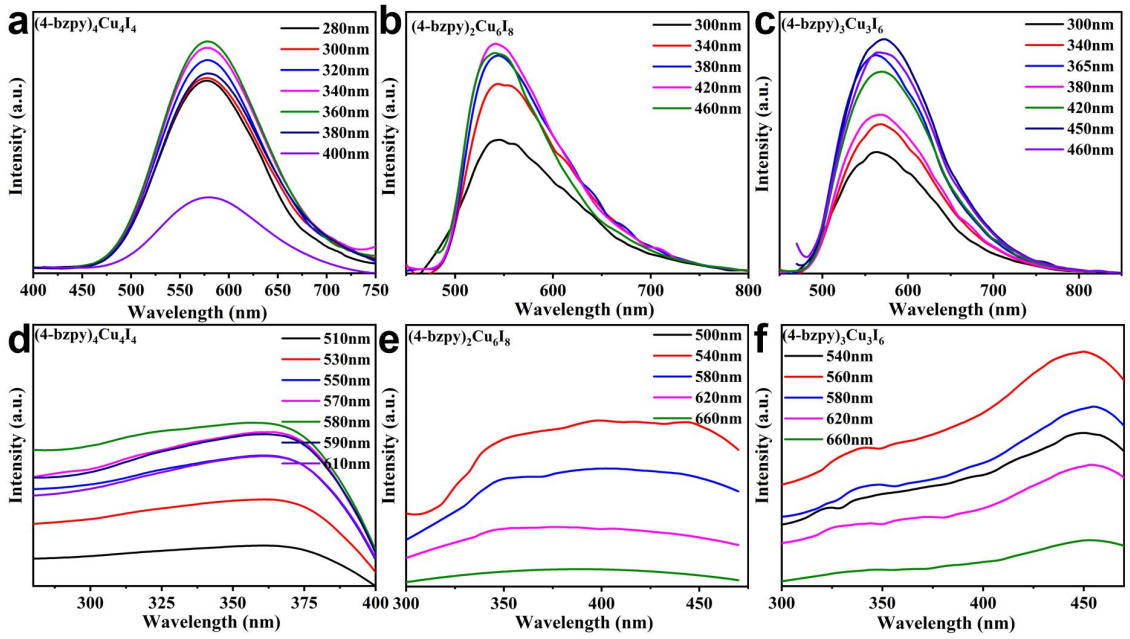

Fig. S3. Excitation and emission-wavelength dependent PL and PLE spectra of $(4\text{-bzpy})_4Cu_4I_4$, $(4\text{-bzpy})_2Cu_6I_8$ and $(4\text{-bzpy})_3Cu_3I_6$ single crystals at room temperature.

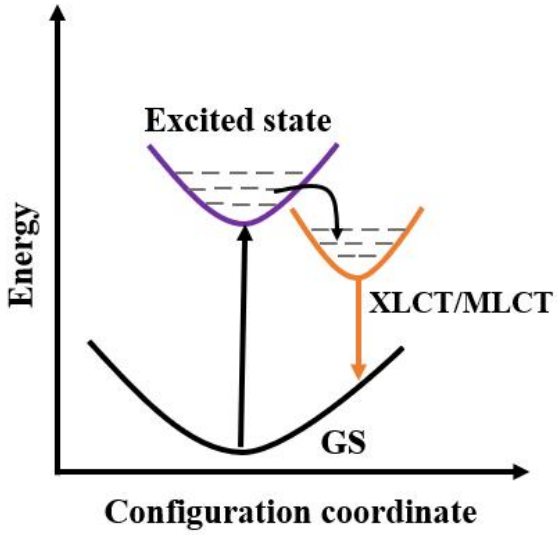

Fig. S4. Coordinate diagram displaying photophysical processes in $(4\text{-bzpy})_4Cu_4I_4$ single crystal.

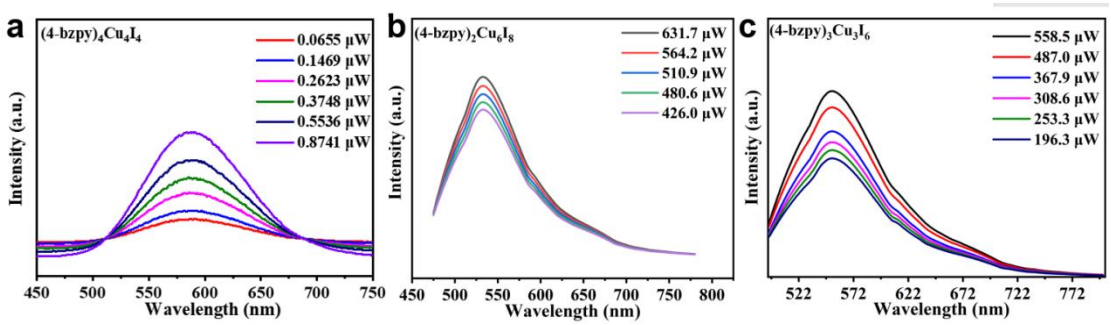

Fig. S5. PL intensity versus excitation power for $(4\text{-bzpy})_4Cu_4I_4$, $(4\text{-bzpy})_2Cu_6I_8$ and $(4\text{-bzpy})_3Cu_3I_6$.

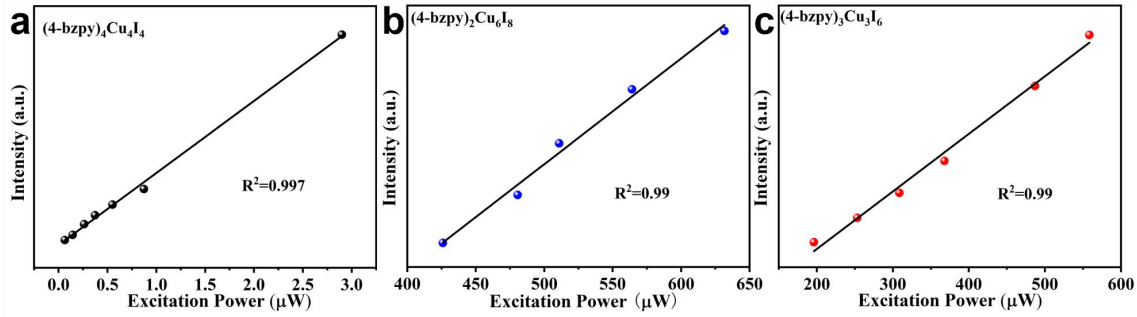

Fig. S6. Integrated PL intensity versus excitation power for $(4\text{-bzpy})_4Cu_4I_4$, $(4\text{-bzpy})_2Cu_6I_8$ and $(4\text{-bzpy})_3Cu_3I_6$.

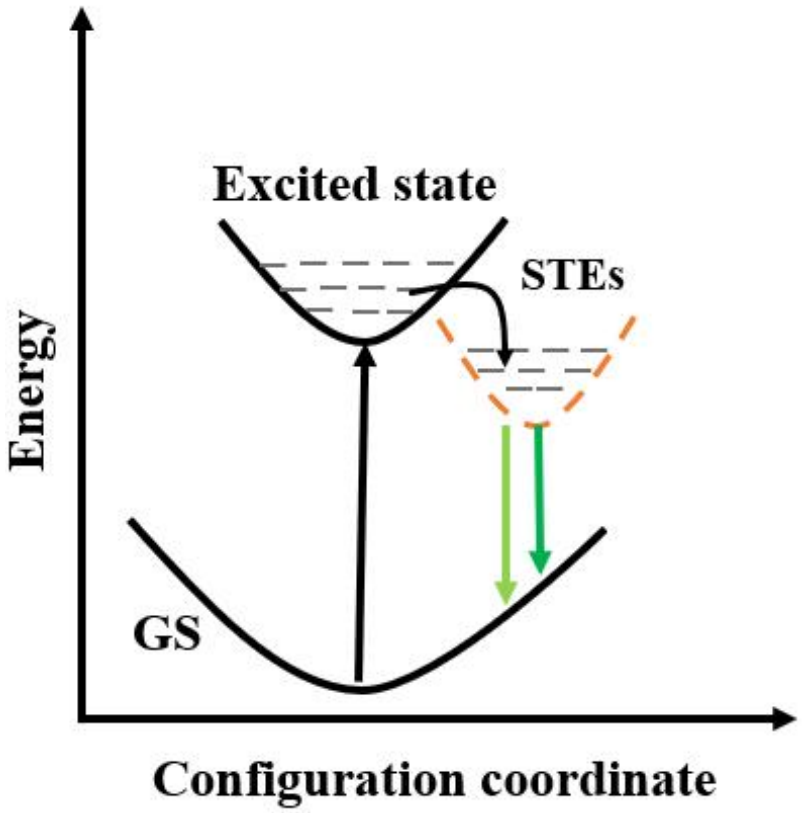

Fig. S7. Coordinate diagram displaying photophysical processes in $(4\text{-bzpy})_2Cu_6I_8$ and $(4\text{-bzpy})_3Cu_3I_6$ single crystal.

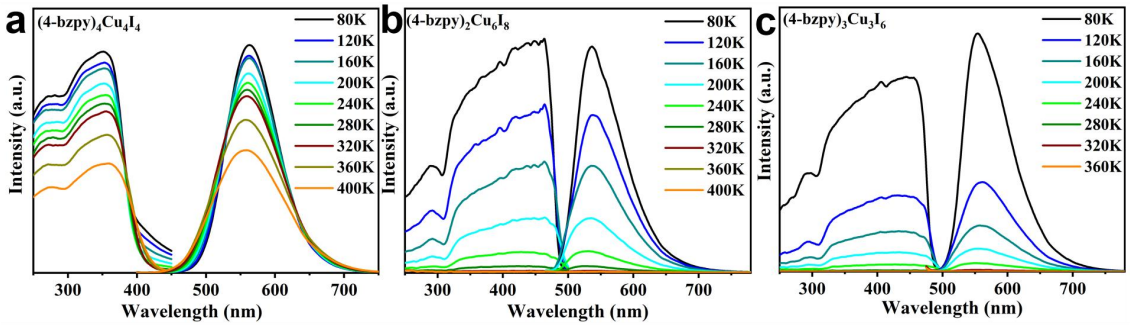

Fig. S8. Temperature-dependent PL spectra of the $(4\text{-bzpy})_4Cu_4I_4$, $(4\text{-bzpy})_2Cu_6I_8$ and $(4\text{-bzpy})_3Cu_3I_6$.

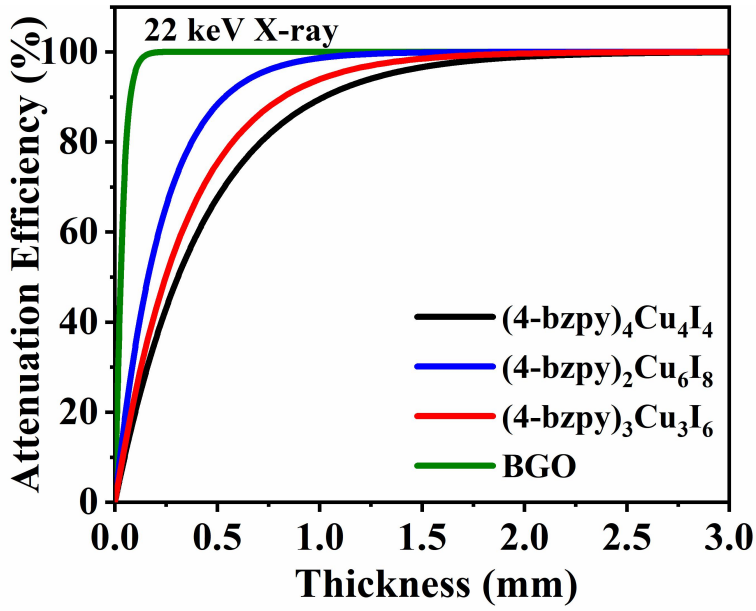

Fig. S9. Attenuation efficiency of $(4\text{-bzpy})_4Cu_4I_4$, $(4\text{-bzpy})_2Cu_6I_8$, $(4\text{-bzpy})_3Cu_3I_6$, and BGO scintillators as a function of 22 keV photon energy.

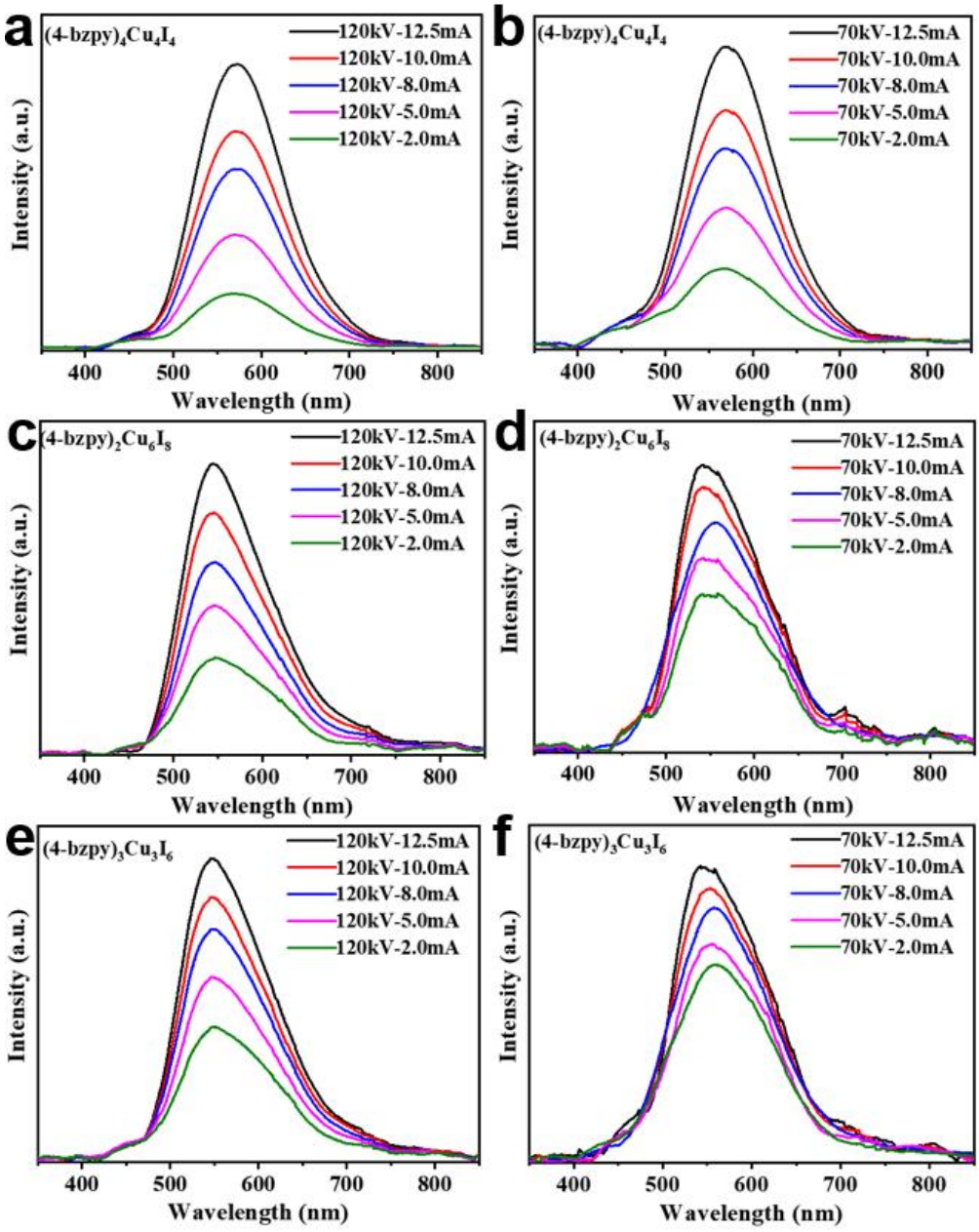

Fig. S10. Emission intensity of $(4\text{-bzpy})_4Cu_4I_4$, $(4\text{-bzpy})_2Cu_6I_8$ and $(4\text{-bzpy})_3Cu_3I_6$ powders using different X-ray dose rates at different kV (70 kV,120 kV) values.

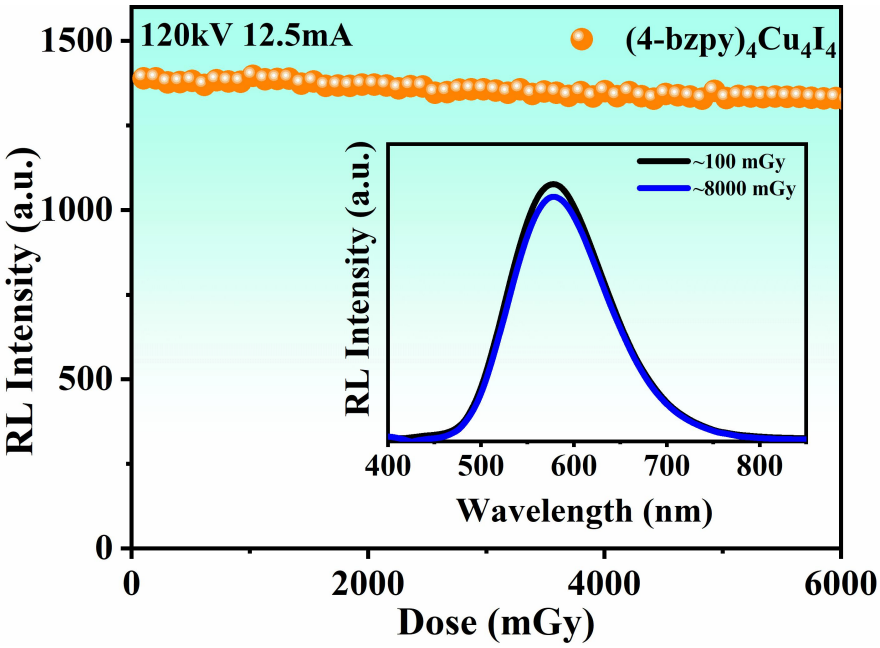

Fig. S11. RL intensity of $(4\text{-bzpy})_4Cu_4I_4$ under continuous X-ray irradiation with a total dose of 8.3 Gy. The inset shows the RL intensity at the first and 78th irradiation.

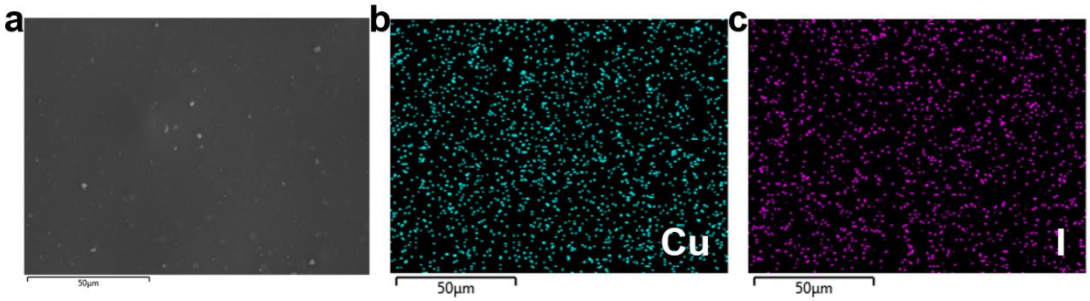

Fig. S12. SEM photograph and elemental mappings of Cu and I atoms in the $(4\text{-bzpy})_4Cu_4I_4$ scintillator film.

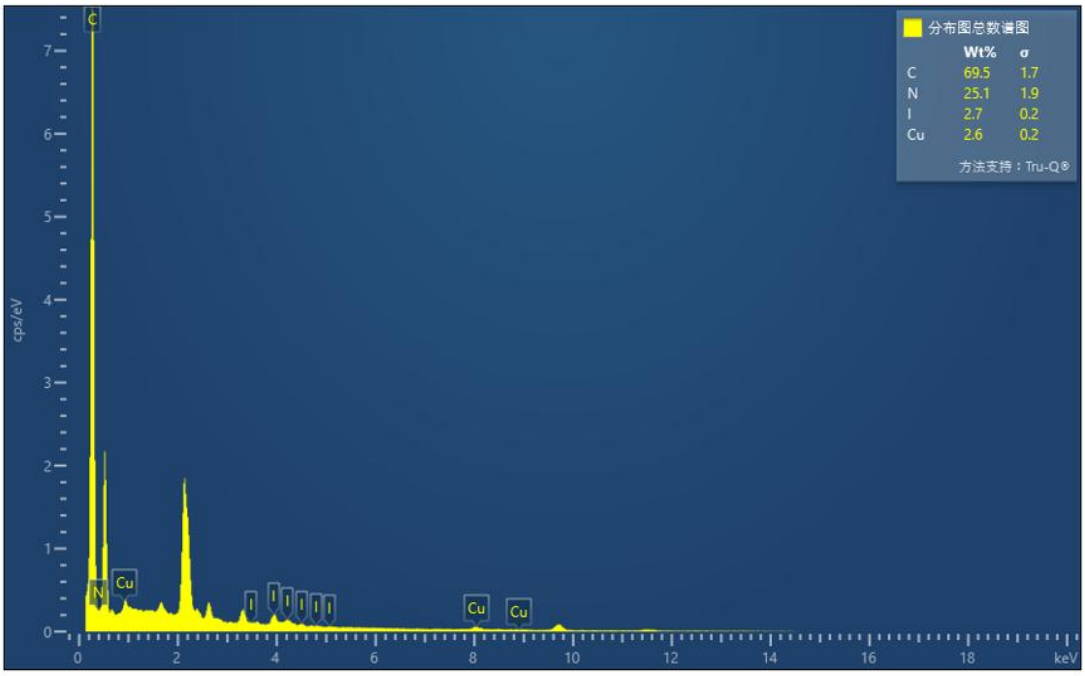

Fig. S13. EDS spectra and element ratio in SEM images of $(4\text{-bzpy})_4Cu_4I_4$ scintillator film.

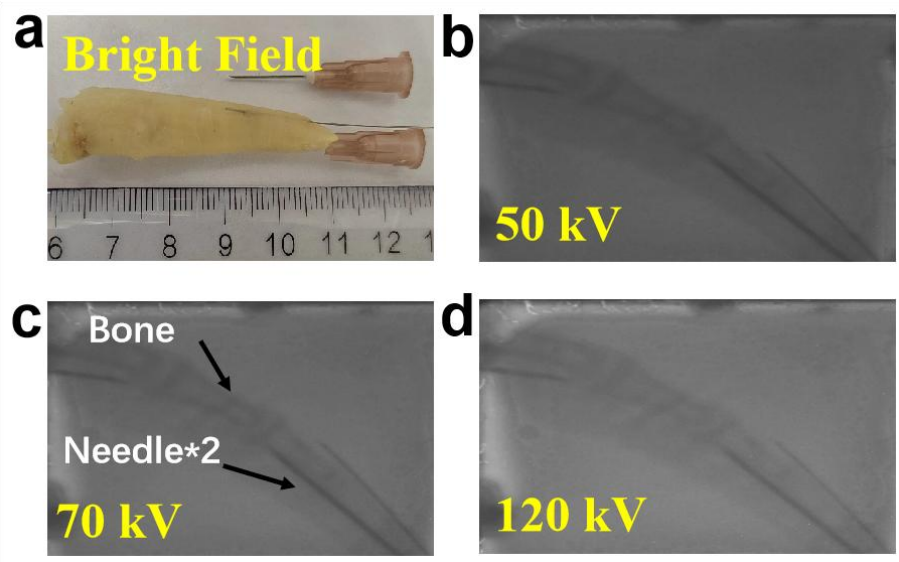

Fig. S14. Photos and corresponding X-ray images at different kV values of chicken feet and the needles under the skin.

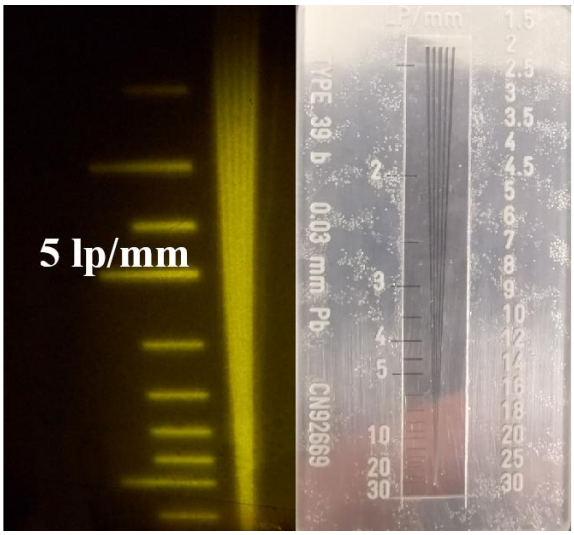

Fig. S15. Photos and X-ray images of standard line-pair card.